Full Articles

Radical character of non-IPR isomer 28324 of C_{80} fullerene

A. R. Khamatgalimov,[a]★ I. V. Petrovicheva,[b] and V. I. Kovalenko[a]

[a]A. E. Arbuzov Institute of Organic and Physical Chemistry, Kazan Scientific Center of the Russian Academy of Sciences, 8 ul. Akad. Arbuzova, 420088 Kazan, Russian Federation. Fax: +7 (843) 273 2253. E-mail: ayrat_kh@iopc.ru
[b]Kazan National Research Technological University, 68 ul. Karla Marksa, 420015 Kazan, Russian Federation

The molecular structure of the 28324 isomer (C_1) of C_{80} fullerene was analyzed based on the concept of substructures in fullerene molecules and with allowance for results of relevant quantum chemical calculations. The distribution of single, double, and delocalized π-bonds is presented for the first time. It is shown that the instability of the fullerene studied is due to its open-shell structure and high local strain. It was found that positions of endohedral metal atoms inside the fullerene cage are in the region of the radical cluster discovered.

Key words: isolated pentagon rule, molecular structure, distribution of chemical bonds, substructures, endohedral metallofullerene, quantum chemical calculations.

According to the isolated pentagon rule (IPR), the most stable fullerenes are those having no fused pentagon pairs, the non-IPR fullerenes being unstable.[1,2] The terms "instability" and "unstable fullerene" imply that it is impossible to obtain a pristine fullerene using currently available synthetic procedures. Until now, there is no reliable confirmation of obtaining such structures as pristine fullerenes. Although about 100 higher non-IPR fullerenes have been reported to date, they represent either *endo*- or *exo*-derivatives.[3] Another unsolved problem is the search for a relation between the structure of the starting fullerene molecule and positions of endohedral atoms inside the fullerene cage or positions of addends outside the cage. A possible reason for this uncertainty is the lack of information on the molecular structure of higher fullerenes.

Our "substructural" concept proved to be useful to study the stability of higher IPR-fullerenes.[4—7] Using reasonable assumptions based on detailed analysis of reliable experimental data on fullerenes, it is possible to obtain a tentative structural formula of the fullerene molecule under study, that is, to establish the distribution of the simple, double, and delocalized bonds prior to calculations. This treatment essentially simplified subsequent analysis of the geometry and electronic structure of the molecule using the results of quantum chemical calculations. Earlier, this approach was used to predict the stability of certain C_{84} fullerene[4] isomers that were isolated more recently.[8,9]

The essence of the concept is to choose a fragment (substructure) of a fullerene molecule, which is bound to the remaining part of the molecule by a simple bond. We

Published in Russian in *Izvestiya Akademii Nauk. Seriya Khimicheskaya,* No. 9, pp. 1651—1656, September, 2021.
1066-5285/21/7009-1651

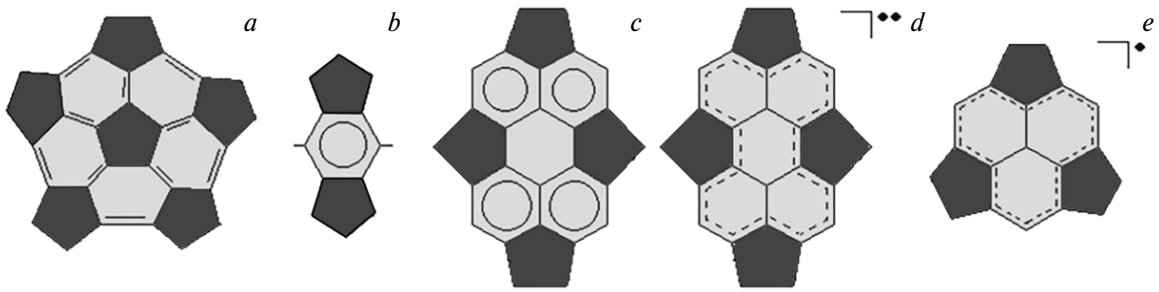

Fig. 1. Characteristic substructures in fullerene molecules: corannulene (*a*), s-indacene (*b*), perylene (*c*, *d*), and phenalenyl radical (*e*).

assume that the main features of the substructure are retained irrespective of the type of the fullerene molecule it belongs to. An analysis of the structure of higher IPR-fullerenes revealed not only substructures characteristic of stable fullerene molecules (Fig. 1, *a* and *b*), but also numerous radical-type substructures (Fig. 1, *d* and *e*) typical of unstable IPR-fullerenes.[5,6]

As can be seen, the perylene substructure can be treated as a closed-shell substructure having no radical centers (Fig. 1, *c*) or as a possible radical substructure consisting of two phenalenyl radical substructures (see Fig. 1, *e*) with a shared hexagon (see Fig. 1, *d*).

According to the structural data obtained mainly by single-crystal X-ray diffraction, a large fraction of IPR-fullerenes are represented by endo- or exohedral derivatives (see, *e.g.*, Refs 10—24). It was found that all of them contain either the phenalenyl radical or perylene substructures as evidenced by our previous studies on C_{74}—C_{86} fullerenes.[5,6] This actually indicates a radical character of these molecules, implying that they are unstable or that it is impossible to obtain them as pristine fullerenes. As to the non-IPR fullerenes, it is the presence of fused pentagons that is the main reason for their instability.

In this work, our "substructural" approach[5—7] is applied to higher non-IPR fullerenes taking the 28324 isomer (C_1) of C_{80} fullerene (isomer numbering is according to the spiral algorithm[25]) as an example. Recently,[26] this species was obtained as endohedral fullerenes U@C_{80} and Th@C_{80} and characterized by single-crystal X-ray diffraction. Our goal was to elucidate structural features of non-IPR fullerene molecules that are responsible for instability of these systems and to provide insight into the reasons for stabilization of such fullerenes as endo- or exo-derivatives.

Calculation Procedure

Our approach allows one to obtain the structural formula of the fullerene molecule and to assess the distribution of all types of bonds (simple, double, delocalized) prior to quantum chemical calculations. This approach was used to analyze a wide range of higher IPR-fullerenes from C_{72} to C_{86} (see Refs 4—6) as well as certain isomers of two lower fullerenes, C_{40} and C_{50},[27—29] and to assess the stability of these molecules. Then, to evaluate preliminary results and to obtain additional structural information, DFT calculations without symmetry restrictions were carried out using the B3LYP functional[30,31] and the 6-31G basis set. The total energies were also revised using the 6-31G* and 6-31+G* extended basis sets. Since the 28324 (C_1) isomer of C_{80} fullerene was also treated as an open-shell structure, we carried out spin-unrestricted Kohn—Sham calculations for high-multiplicity configurations. All calculations were carried out using the Gaussian 09 program.[32] The calculations and a normal vibration analysis confirmed the correspondence between the optimized structures and the energy minima located on the potential energy surfaces.

Results and Discussion

Consider the distribution of simple, double, and delocalized π-bonds in the 28324 isomer (C_1) of C_{80} fullerene (Fig. 2) from the standpoint of our approach.[4—7] An analysis of the structural formula revealed the presence of corannulene substructures (see Fig. 1, *a*) characteristic of both the most stable fullerenes C_{60} and C_{70} and other stable IPR-fullerenes. These substructures cannot cause the instability of the molecule under study.

Of particular interest is a cluster consisting of three fused phenalenyl radical substructures and phenanthrene (see Fig. 2). This cluster is identical to a cluster in the IPR-isomer 39715 (C_s) of the C_{82} fullerene that was obtained and characterized only as various endohedral derivatives[5,6,11,19—21] rather than a pristine fullerene. In the molecule of the title isomer this cluster is adjacent to the pentalene moiety that plays a dual role. First, a recent study[33] showed that certain pentalene derivatives are open-shell systems with two unpaired electrons. Next, the C_8 framework of pentalene and its derivatives is planar, being significantly distorted in the strained fullerene spheroid; earlier, the effect of the curvature of the spheroid was considered as a reason for the instability of pentalene-containing fullerenes. One can expect that the molecule of the 28324 isomer (C_1) of C_{80} fullerene contains a kind of a radical cluster consisting of six "fused" phenalenyl radical substructures and an adjacent pentalene moiety.

Thus, a preliminary analysis of the structure of the 28324 isomer (C_1) of C_{80} fullerene showed that its instabil-

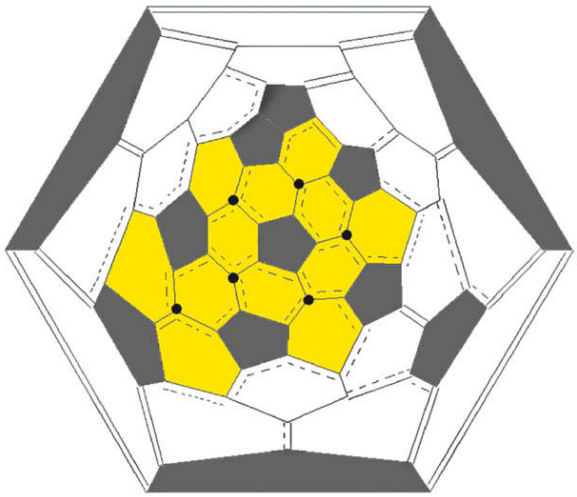

Fig. 2. Schlegel diagram of the open-shell 28324 isomer (C_1) of C_{80} fullerene. The tentative radical cluster is given in yellow. Small filled circles denote the central carbon atoms of six "fused" phenalenyl radical substructures. Here and in Figs 4 and 5 single lines denote the simple bonds, double lines denote the double bonds, and dashed lines denote the delocalized π-bonds.

ity can be due to the radical character and a local strain produced by the pentalene fragment.

To evaluate the preliminary results obtained and to determine the character of the electronic structure of the isomer under study, we carried out quantum chemical calculations for different-multiplicity (M) configurations including those with two and four unpaired electrons (M = 3 and 5, respectively). Calculations revealed the closed-shell singlet configuration (Table 1) as the most energetically favorable one. Nevertheless, the high-multiplicity (triplet and quintet) configurations were also analyzed taking account of the arguments for the radical character of the electronic structure of the fullerene in hand (see above).

It was found that although the energies of the configurations with $M = 3$ and 5 are respectively 6 and 18 kcal mol^{-1} higher than that of the singlet configuration, this energy difference is compensated by a considerable energy gain for ionic forms. The C_{80}^{4-} and C_{80}^{6-} anions of the 28324 isomer (C_1) of C_{80} fullerene become even more energetically favorable than the most stable 31919 isomer (D_2) of the IPR-fullerene C_{80} (Table 2).

In fact, the results of DFT calculations confirmed the preliminary bond distribution obtained using our approach,[4–7] *viz.*, most calculated bond lengths correspond to the expected bond types (simple, double, and delocalized), being close to the bond lengths in the well-studied fullerenes C_{60} and C_{70} (Table 3 and Fig. 3). On going to the anions the lengths of the simple bonds remain almost unchanged, while the double and delocalized bonds become somewhat longer.

Nevertheless, differences between the results of calculations and the values expected from the preliminary bond distribution merit attention. It was found that most delocalized bonds correspond to the phenalenyl radical substructures and their positions in the configurations with $M = 3$ and 5 differ only slightly. Therefore, determination of the number of unpaired electrons requires an analysis of the spin density distribution in different configurations.

Table 1. Relative energies (ΔE) of and HOMO—LUMO gaps ($\Delta E_{HOMO-LUMO}$) in isomers of C_{80} fullerene

Isomer	M^a	ΔE/kcal mol^{-1}			$\Delta E_{HOMO-LUMO}$/eV		
		6-31G	6-31G*	6-31+G*	6-31G	6-31G*	6-31+G*
31919 (D_2)[b]	1	0.00	0.00	0.00	1.39	1.35	1.33
28324 (C_1)	1	28.99	27.00	26.14	1.16	1.16	1.16
	3	34.76	33.02	32.38	0.66	0.66	0.65
	5	47.50	45.13	44.39	0.34	0.37	0.36

[a] M is the multiplicity of the corresponding electronic configuration.
[b] The most stable IPR isomer of C_{80} fullerene.[34]

Table 2. Relative energies (ΔE, kcal mol^{-1}) and HOMO—LUMO gaps ($\Delta E_{HOMO-LUMO}$, eV) in anions of the 31919 (D_2) and 28324 (C_1) isomers of C_{80} fullerene

Isomer	C_{80}		C_{80}^{2-}		C_{80}^{4-}		C_{80}^{6-}	
	ΔE	$\Delta E_{HOMO-LUMO}$	ΔE	$\Delta E_{HOMO-LUMO}$	ΔE	$\Delta E_{HOMO-LUMO}$	ΔE	$\Delta E_{HOMO-LUMO}$
31919 (D_2)[a]	0.00	1.33	0.00	1.29	0.00	0.86	0.00	1.13
28324 (C_1)	26.14	1.16	11.03	0.96	−17.81	1.27	−23.51	1.28

[a] The most stable IPR isomer of C_{80} fullerene.[34]

Table 3. The minimum (l_{min}), average (l_{av}), and maximum (l_{max}) lengths (Å) of simple, double, and delocalized bonds in the fullerenes C_{60} (I_h) and C_{70} (D_{5h}), in the 28324 isomer (C_1) of C_{80} fullerene in different electronic configurations, and in the endohedral metallofullerenes U@C_{80}(28324) and Th@C_{80}(28324)

Fullerene	Simple			Double			Delocalized		
	l_{min}	l_{av}	l_{max}	l_{min}	l_{av}	l_{max}	l_{min}	l_{av}	l_{max}
C_{60} (I_h)[a]	—	1.4580	—	—	1.401	—	—	—	—
C_{70} (D_{5h})[b]	1.4530	—	1.5310	1.3860	—	1.3880	1.4050	—	1.4250
C_{80} 28324 (C_1), singlet[c]	1.4210	1.4536	1.4815	1.3669	1.3965	1.4153	1.4007	1.4298	1.4649
C_{80} 28324 (C_1), triplet[c]	1.4196	1.4539	1.4821	1.3705	1.3963	1.4149	1.3974	1.4301	1.4682
C_{80} 28324 (C_1), quintet[c]	1.4404	1.4552	1.4745	1.3736	1.4000	1.4205	1.4032	1.4274	1.4662
C_{80}^{2-} 28324 (C_1)[c]	1.4292	1.4555	1.4953	1.3731	1.3991	1.4148	1.3977	1.4307	1.4619
C_{80}^{4-} 28324 (C_1)[c]	1.4360	1.4553	1.4786	1.3893	1.4084	1.4307	1.4138	1.4347	1.4494
C_{80}^{6-} 28324 (C_1)[c]	1.4308	1.4564	1.4837	1.3936	1.4233	1.4747	1.4241	1.4347	1.4659
U@C_{80}(28324)[d]	1.4273	1.4473	1.4685	1.3796	1.4037	1.4437	1.4118	1.4293	1.4615
Th@C_{80}(28324)[d]	1.4275	1.4480	1.4715	1.3809	1.4044	1.4470	1.4111	1.4297	1.4654

[a] Gas-phase electron diffraction data.[35]
[b] Gas-phase electron diffraction data.[36]
[c] Obtained from B3LYP/6-31G calculations.
[e] X-ray diffraction data.[26]

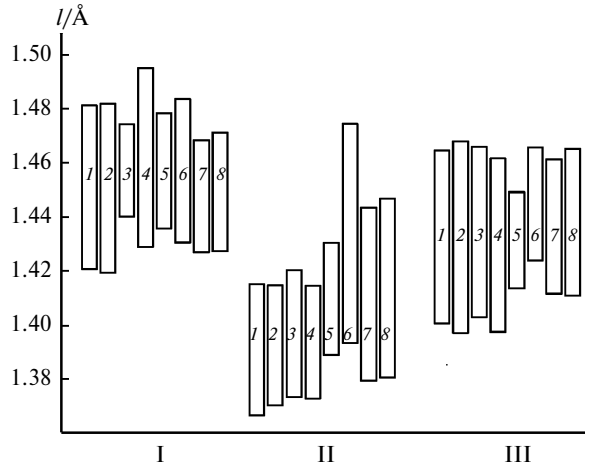

Fig. 3. Minimum and maximum bond length (in Å) distribution for the simple (I), double (II), and delocalized (III) bonds: singlet C_{80}(28324) (*1*), triplet C_{80}(28324) (*2*), quintet C_{80}(28324) (*3*), C_{80}^{2-}(28324) (*4*), C_{80}^{4-}(28324) (*5*), C_{80}^{6-}(28324) (*6*), U@C_{80}(28324) (*7*), and Th@C_{80}(28324) (*8*).

As was expected, the spin density in all electronic configurations is mainly localized on atoms of the radical cluster (Fig. 4). Note that the quintet configuration is the preferred one since it is this configuration that provided localization of the highest spin density on the radical cluster and pentalene moiety (see Ref. 33).

Positions of metal atom(-s) inside the cage of endohedral fullerenes are specified by the spin density distribution. Earlier, we found that metal cations are located near the spin-density-rich radical substructures of the parent fullerene.[37]

Our structural data for the 28324 isomer (C_1) of C_{80} fullerene were compared with the experimental data for the endohedral metallofullerenes U@C_{80}(28324) and Th@C_{80}(28324) obtained by single-crystal X-ray diffraction.[26] Positions of endohedral thorium and uranium atoms are in the region of the radical cluster and pentalene moiety (Fig. 5). This confirms our assumption that endohedral atoms are located near the radical clusters since it is these regions that are characterized by the maximum spin density. Taking into account the fact that the endohedral Th and

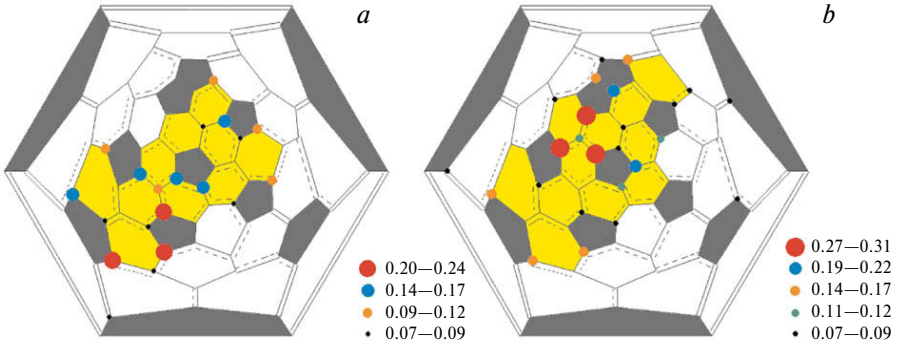

Fig. 4. Maximum spin density distribution in the 28324 isomer (C_1) of C_{80} fullerene for the configurations with two (*a*) and four (*b*) unpaired electrons; the highest spin density region is given in yellow.

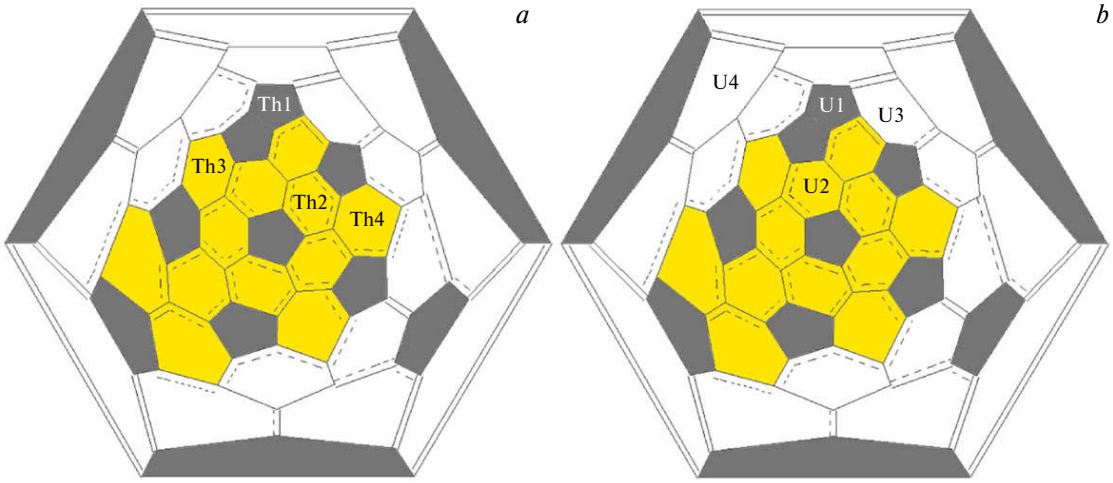

Fig. 5. Positons of endohedral atoms in Th@C_{80} (*a*) and U@C_{80} (*b*) near the pentalene and phenalenyl radical substructures. The highest spin density region is given in light gray.

U atoms are in the oxidation state 4+,[26] the calculated bond lengths in the C_{80}^{4-} tetraanion of the 28324 isomer (C_1) of C_{80} fullerene are in good agreement with the X-ray diffraction data for the endohedral metallofullerenes U@C_{80}(28324) and Th@C_{80}(28324) (see Table 3 and Fig. 3).

Reference can be made to another reason for stabilization of non-IPR endohedral metallofullerenes. Going from planar pentalene structures to folded pentalene substructures in the fullerene molecule produces a considerable local strain.[6,38,39] For instance, the pentalene folding angle in the hypothetical molecule of the 28324 isomer (C_1) of C_{80} fullerene is about 47°. Stabilization of this molecule in the form of endohedral metallofullerenes can be explained by strain relaxation caused by coordination of the endohedral metal cation to the pentalene dianion.[40]

Summing up, the instability of the non-IPR 28324 isomer (C_1) of C_{80} fullerene studied in this work is most probably due to its open-shell structure and high local strain. We have shown that combining our approach to molecular structure determination of higher fullerenes and quantum chemical calculations can also be useful in the structural studies of non-IPR fullerenes.

This work was carried out within the framework of the State Assignment and under partial financial support from the Russian Foundation for Basic Research (Project No. 18-29-19110MK).

This paper does not contain descriptions of studies on animals or humans.

The authors declare no competing interests.

References

1. H. W. Kroto, *Nature*, 1987, **329**, 529; DOI: 10.1038/329529a0.
2. T. G. Schmalz, W. A. Seitz, D. J. Klein, G. E. Hite, *J. Am. Chem. Soc.*, 1988, **110**, 1113; DOI: 10.1021/ja00212a020.
3. R. Guan, M. Chen, F. Jin, S. Yang, *Angew. Chem., Int. Ed.*, 2020, **59**, 1048; DOI: 10.1002/anie.201901678.
4. V. I. Kovalenko, A. R. Khamatgalimov, *Russ. Chem. Rev.*, 2006, **75**, 981; DOI: 10.1070/RC2006v075n11ABEH003620.
5. A. R. Khamatgalimov, V. I. Kovalenko, *Russ. Chem. Rev.*, 2016, **85**, 836; DOI: 10.1070/RCR4571.
6. V. I. Kovalenko, A. R. Khamatgalimov, *Stroenie i stabil'nost' vysshikh fullerenov* [*The Structure and Stability of Higher Fullerenes*], Russian Academy of Sciences, Moscow, 2019, 212 pp. (in Russian).
7. A. R. Khamatgalimov, V. I. Kovalenko, *Int. J. Mol. Sci.*, 2021, **22**, 3760; DOI: 10.3390/ijms22073760.
8. L. Epple, K. Amsharov, K. Simeonov, I. Dix, M. Jansen, *Chem. Commun.*, 2008, 5610; DOI: 10.1039/b811872h.
9. N. Tamm, L. N. Sidorov, E. Kemnitz, S. I. Troyanov, *Chem. Eur. J.*, 2009, **15**, 10486; DOI: 10.1002/chem.200901596.
10. W. Shen, L. Bao, S. Yu, L. Yang, P. Jin, Y. Xie, T. Akasaka, X. Lu, *Chem. Sci.*, 2019, **10**, 829; DOI: 10.1039/c8sc03886d.
11. P. Yu, L. Bao, L. Yang, D. Hao, P. Jin, W. Shen, H. Fang, T. Akasaka, X. Lu, *Inorg. Chem.*, 2020, **59**, 9416; DOI: 10.1021/acs.inorgchem.0c01304.
12. W. Cai, J. Alvarado, A. Metta-Magaña, N. Chen, L. Echegoyen, *J. Am. Chem. Soc.*, 2020, **142**, 13112; DOI: 10.1021/jacs.0c04888.
13. H. Nikawa, T. Yamada, B. Cao, N. Mizorogi, Z. Slanina, T. Tsuchiya, T. Akasaka, K. Yoza, S. Nagase, *J. Am. Chem. Soc.*, 2009, **131**, 10950; DOI: 10.1021/ja900972r.
14. X. Lu, Z. Slanina, T. Akasaka, T. Tsuchiya, N. Mizorogi, S. Nagase, *J. Am. Chem. Soc.*, 2010, **132**, 5896; DOI: 10.1021/ja101131e.
15. N. B. Shustova, I. V. Kuvychko, R. D. Bolskar, K. Seppelt, S. H. Strauss, A. A. Popov, O. V. Boltalina, *J. Am. Chem. Soc.*, 2006, **128**, 15793; DOI: 10.1021/ja065178l.
16. J. C. Duchamp, A. Demortier, K. R. Fletcher, D. Dorn, E. B. Iezzi, T. Glass, H. C. Dorn, *Chem. Phys. Lett.*, 2003, **375**, 655; DOI: 10.1016/S0009-2614(03)00844-3.
17. T. Zuo, M. M. Olmstead, C. M. Beavers, A. L. Balch, G. Wang, G. T. Yee, C. Shu, L. Xu, B. Elliott, L. Echegoyen, J. C. Duchamp, H. C. Dorn, *Inorg. Chem.*, 2008, **47**, 5234; DOI: 10.1021/ic800227x.

18. T. Zuo, C. M. Beavers, J. C. Duchamp, A. Campbell, H. C. Dorn, M. M. Olmstead, A. L. Balch, *J. Am. Chem. Soc.*, 2007, **129**, 2035; DOI: 10.1021/ja066437+.
19. M. M. Olmstead, A. Bettencourt-Dias, S. Stevenson, H. C. Dorn, A. L. Balch, *J. Am. Chem. Soc.*, 2002, **124,** 4172; DOI: 10.1021/ja0116019.
20. B. Q. Mercado, N. Chen, A. Rodríguez-Fortea, M. A. Mackey, S. Stevenson, L. Echegoyen, J. M. Poblet, M. M. Olmstead, A. L. Balch, *J. Am. Chem. Soc.,* 2011, **133,** 6752; DOI: 10.1021/ja200289w.
21. H. Yang, H. Jin, X. Wang, Z. Liu, M. Yu, F. Zhao, B. Q. Mercado, M. M. Olmstead, A. A. Balch, *J. Am. Chem. Soc.,* 2012, **134,** 14127; DOI: 10.1021/ja304867j.
22. R. Guan, F. Jin, S. Yang, N. B. Tamm, S. I. Troyanov, *Inorg. Chem*., 2019, **58**, 5393; DOI: 10.1021/acs.inorgchem.9b00144.
23. S. Yang, I. N. Ioffe, S. I. Troyanov, *Acc. Chem. Res.,* 2019, **52**, 1783; DOI: 10.1021/acs.accounts.9b00175.
24. S. Wang, Q. Chang, G. Zhang, F. Li, X. Wang, S. Yang, S. I. Troyanov, *Front. Chem*., 2020, **8**, 607712; DOI: 10.3389/fchem.2020.607712.
25. P. W. Fowler, D. E. Manolopoulos, *An Atlas of Fullerenes,* Dover Publ., Mineola, New York, 2006, 392 pp.
26. W. Cai, L. Abella, J. Zhuang, X. Zhang, L. Feng, Y. Wang, R. Morales-Martínez, R. Esper, M. Boero, A. Metta-Magaña, A. Rodríguez-Fortea, J. M. Poblet, L. Echegoyen, N. Chen, *J. Am. Chem. Soc*., 2018, **140**, 18039; DOI: 10.1021/jacs.8b10435.
27. A. R. Khamatgalimov, R. I. Idrisov, I. I. Kamaletdinov, V. I. Kovalenko, *Mendeleev Commun*., 2020, **30**, 725; DOI: 10.1016/j.mencom.2020.11.012.
28. A. R. Khamatgalimov, R. I. Idrisov, I. I. Kamaletdinov, V. I. Kovalenko, *J. Mol. Model*., 2021, **27**, 22; DOI: 10.1007/s00894-020-04625-9.
29. A. R. Khamatgalimov, L. I. Yakupova, V. I. Kovalenko, *Theor. Chem. Acc*., 2020, **139**, 159; DOI: 10.1007/s00214-020-02675-z.
30. A. D. Becke, *J. Chem. Phys.*, 1993, **98**, 5648; DOI: 10.1063/1.464913.
31. C. Lee, W. Yang, R. G. Parr, *Phys. Rev. B*, 1988, **37**, 785; DOI: 10.1103/PhysRevB.37.785.
32. M. J. Frisch, G. W. Trucks, H. B. Schlegel, G. E. Scuseria, M. A. Robb, J. R. Cheeseman, G. Scalmani, V. Barone, B. Mennucci, G. A. Petersson, H. Nakatsuji, M. Caricato, X. Li, H. P. Hratchian, A. F. Izmaylov, J. Bloino, G. Zheng, J. L. Sonnenberg, M. Hada, M. Ehara, K. Toyota, R. Fukuda, J. Hasegawa, M. Ishida, T. Nakajima, Y. Honda, O. Kitao, H. Nakai, T. Vreven, J. A. Montgomery, Jr., J. E. Peralta, F. Ogliaro, M. Bearpark, J. J. Heyd, E. Brothers, K. N. Kudin, V. N. Staroverov, R. Kobayashi, J. Normand, K. Raghavachari, A. Rendell, J. C. Burant, S. S. Iyengar, J. Tomasi, M. Cossi, N. Rega, J. M. Millam, M. Klene, J. E. Knox, J. B. Cross, V. Bakken, C. Adamo, J. Jaramillo, R. Gomperts, R. E. Stratmann, O. Yazyev, A. J. Austin, R. Cammi, C. Pomelli, J. W. Ochterski, R. L. Martin, K. Morokuma, V. G. Zakrzewski, G. A. Voth, P. Salvador, J. J. Dannenberg, S. Dapprich, A. D. Daniels, O. Farkas, J. B. Foresman, J. V. Ortiz, J. Cioslowski, D. J. Fox, *Gaussian 09*, *Revision A.1*, Gaussian, Inc., Wallingford CT, 2009.
33. A. Konishi, Y. Okada, M. Nakano, K. Sugisaki, K. Sato, T. Takui, M. Yasuda, *J. Am. Chem. Soc*., 2017, **139**, 15284; DOI: 10.1021/jacs.7b05709.
34. A. R. Khamatgalimov, V. I. Kovalenko, *J. Phys. Chem. A*., 2011, **115**, 12315; DOI: 10.1021/jp204565q.
35. K. Hedberg, L. Hedberg, D. S. Bethune, C. A. Brown, H. C. Dorn, R. D. Johnson, M. de Vries, *Science*, 1991, **254**, 410; DOI: 10.1126/science.254.5030.410.
36. K. Hedberg, L. Hedberg, M. Buhl, D. S. Bethune, C. A. Brown, R. D. J. Johnson, *J. Am. Chem. Soc.,* 1997, **119**, 5314; DOI: 10.1021/ja970110e.
37. A. R. Khamatgalimov, V. I. Kovalenko, *Fuller. Nanotub. Car. Nanostruct.,* 2011, **19**, 599; DOI: 10.1080/1536383X.2010.504951.
38. Y.-Z. Tan, S.-Y. Xie, R.-B. Huang, L.-S. Zheng, *Nature Chem*., 2009, **1**, 450; DOI: 10.1038/nchem.329.
39. Q. Deng, A. A. Popov, *J. Am. Chem. Soc*., 2014, **136**, 4257; DOI: 10.1021/ja4122582.
40. O. T. Summerscales, F. G. N. Cloke, *Coord. Chem. Rev*. 2006, **250**, 1122; DOI: 10.1016/j.ccr.2005.11.020.

Received November 30, 2020;
in revised form February 15, 2021;
accepted April 12, 2021